Journal of Computational and Applied Mathematics 39 (1992) 353–361
North-Holland

Applications of von Mises coordinates in porous media flow

M.H. Hamdan *
Department of Mathematics & Computer Science, Mount Allison University, Sackville, New Brunswick, Canada E0A 3C0

R.M. Barron
Department of Mathematics & Statistics, and Fluid Dynamics Research Institute, University of Windsor, Windsor, Ontario, Canada N9B 3P4

Received 2 October 1990

Abstract

Hamdan, M.H. and R.M. Barron, Applications of von Mises coordinates in porous media flow, Journal of Computational and Applied Mathematics 39 (1992) 353–361.

Numerical implementation of the von Mises transformation in porous media flow has been illustrated using the Darcy model. Flow through a semi-finite porous block bounded below by an impermeable wall of arbitrary shape has been analysed by a finite-difference method. The use of the von Mises transformation eliminates any need to numerically generate a grid system.

Keywords: Porous media, Darcy's law, von Mises transformation, curved boundaries.

1. Introduction

The study of fluid flow through porous media has become a topic of increasing importance due to its direct applicability in many physical situations including the prediction of oil reservoir behaviour, groundwater flow and irrigation problems [4,6,8] and the biophysical sciences [3,7], where the human lungs, for example, are modelled as porous layers. These and other important applications stress the fundamental importance of seeking solutions to boundary value and initial-value problems in this field.

Depending on the type of the porous structure, on the type of flow and the flow domain considered, the solution methodology for a given boundary value problem has ranged from analytical or semi-analytical methods to numerical solutions that have become possible with the advent of high-speed digital machines. Numerical solutions have gained attention because of

* Present address: Division of Mechanics, University of New Brunswick, P.O. Box 5050, Saint John, New Brunswick, Canada E2L 4L5.

the difficulty in obtaining analytical solutions to the complicated flow problems through porous media. Numerical methods offer more generality in dealing with different boundary conditions, but obtaining numerical solutions is often hindered by the irregular shape of the flow domain, particularly finite-difference solutions. In this case one must resort to techniques such as numerical grid generation or the finite-element method, which has recently gained popularity in the treatment of flow problems in porous media [2].

Although finite differences offer an attractive approach in the study of flow through porous media, they possess a serious drawback in handling cases where the boundaries are arbitrarily curved. A method which is designed to overcome this limitation is presented in this study. The approach is based on transforming the governing equations using the von Mises transformation and the numerical solution is obtained in the computational domain through the use of the finite-difference technique. This formulation was first introduced by Barron [1] in his study of flow over airfoils of arbitrary shape and in the design problem of airfoils. Some of the advantages of the approach were discussed in [1] and include the transformation of any smooth streamline boundary, although curved, into a straight line. This eliminates the difficulties of implementing finite differences in cases with curved boundaries.

The easy implementation of this method makes it more favourable than numerical grid generation. Furthermore, since the occurrence of natural porous media is arbitrary in shape and a given flow domain is likely to have curved boundaries, this method of approach seems to be advantageous in dealing with flow problems in porous media.

2. Governing equations

We consider the two-dimensional flow of an incompressible, homogeneous, viscous fluid through an isotropic porous medium of constant permeability. The structure of the medium is assumed to be one in which Darcy's law is applicable and the flow is assumed to be of seepage type. This flow is governed by the equation of continuity and Darcy's law, i.e.,

$$\nabla \cdot \boldsymbol{u} = 0 \tag{1}$$

and

$$\boldsymbol{u} = -\frac{k}{\mu}\nabla p, \tag{2}$$

where $\boldsymbol{u}$ is the Darcy velocity vector, p is the interstitial pressure, μ is the coefficient of viscosity and k is the permeability.

We introduce the streamfunction ψ, defined in terms of the horizontal and vertical components of velocity u and v, by

$$u = \frac{\partial \psi}{\partial y}, \qquad v = -\frac{\partial \psi}{\partial x}. \tag{3}$$

The equation for the streamfunction, obtained by taking the curl of (2), is

$$\frac{\partial^2 \psi}{\partial x^2} + \frac{\partial^2 \psi}{\partial y^2} = 0. \tag{4}$$

The solution to a given boundary value problem can be obtained by solving (4) for ψ. The velocity components can then be obtained from (3), once ψ is known. The pressure p is related to the velocity by (2), and thus once $\boldsymbol{u}$ is determined, p can be found, for a given permeability and viscosity. The pressure also satisfies the Laplace equation

$$\nabla^2 p = 0. \tag{5}$$

The above equations can be considered dimensionless where velocity and length have been rendered dimensionless with respect to a characteristic speed U_∞ and a characteristic length L.

3. The von Mises transformation

Although the von Mises transformation has been in existence for over half a century, its implementation in the numerical solution of fluid flow problems over airfoils has only recently been investigated by Barron [1]. He arrived at the von Mises transformation through Martin's approach [5] by a judicious choice of the ϕ-curves. In this paper, the applicability of the von Mises transformation in the study of fluid flow through porous media is illustrated by considering the problem of flow through a semi-infinite medium that is bounded below by a curved impermeable wall. The shape of this lower boundary is given in the (x, y)-plane, in general, by

$$y = f(x). \tag{6}$$

In order to solve the governing equations we consider a transformation of coordinates between the Cartesian coordinates (x, y) and the curvilinear coordinates (ϕ, ψ), defined by

$$x = \phi, \qquad y = y(\phi, \psi). \tag{7}$$

The spatial Jacobian of the transformation is given by

$$J = \frac{\partial(x, y)}{\partial(\phi, \psi)} = y_\psi. \tag{8}$$

It is clear that if $J = 0$ or is infinite, then the transformation is singular. If, however, $0 < |J| < \infty$, then (7) defines a one-to-one transformation.

From (3) and results in the Appendix it is easily seen that the velocity components in the new coordinate system are

$$u = \frac{1}{y_\psi}, \qquad v = \frac{y_\phi}{y_\psi}. \tag{9}$$

For convenience of notation we replace ϕ by x. Using the results in the Appendix, the streamfunction equation (4) is transformed to an equation for the variable y in the form

$$y_\psi^2 y_{xx} - 2 y_x y_\psi y_{x\psi} + \left(1 + y_x^2\right) y_{\psi\psi} = 0, \tag{10}$$

while (6) for the pressure takes the form

$$y_\psi^2 p_{xx} - 2 y_x y_\psi p_{x\psi} + \left(1 + y_x^2\right) p_{\psi\psi} = 0. \tag{11}$$

In the von Mises coordinate system, the pressure and velocity components are related by

$$\frac{\mu}{k}u = -p_x + \frac{y_x}{y_\psi}p_\psi, \tag{12}$$

$$\frac{\mu}{k}v = -\frac{1}{y_\psi}p_\psi. \tag{13}$$

With this formulation the problem has been transformed from that of solving (4) for $\psi(x, y)$ and (5) for $p(x, y)$ to that of solving (10) for $y(x, \psi)$ and (11) for $p(x, \psi)$. Although the nonlinear equations (10) and (11) are more complicated than the linear equations (4) and (5), the problem is simplified when dealing with a curved lower boundary, defined by (6). This simplification relies on the fact that this boundary remains a streamline of the flow and hence an irregularly shaped physical domain $-\infty < x < \infty$, $f(x) \leqslant y < \infty$ has been mapped to a rectangular computational domain $-\infty < x < \infty$, $0 \leqslant \psi < \infty$. Furthermore, (10) involves the determination of $y(x, \psi)$ which satisfies a Dirichlet condition at the boundary, assuming that the equation of the lower boundary is given.

4. Boundary conditions and method of solution

The physical (x, y)-plane has been transformed, through the von Mises transformation, into a rectangular computational (x, ψ)-plane. This transformation is unique provided that the sign of the spatial Jacobian of the transformation J does not change throughout the flow field. Given the equation of the lower boundary $y = f(x)$, which is taken as the streamline in the physical plane on which $\psi = 0$, the boundary conditions associated with (10) are

$$\begin{aligned} y &= \psi, && \text{at } x = \pm\infty, && \text{for all } \psi \geqslant 0,\\ y &= \psi, && \text{at } \psi = \infty, && \text{for all } x,\\ y &= f(x), && \text{at } \psi = 0. \end{aligned} \tag{14}$$

The first two conditions imply uniform flow at infinity. The last condition is the flow tangency condition which is valid when the porous medium is of the type where Darcy's law is valid and, in this case, the normal component of velocity is taken to be continuous at the lower curved boundary and is expressed as $\boldsymbol{u} \cdot \boldsymbol{n} = 0$, where $\boldsymbol{n}$ is the unit normal vector to the impermeable wall.

Following [1], equation (10) is solved iteratively by locally freezing the coefficients and central differencing second-order derivatives. The iterative solution to the resulting matrix equation is obtained via successive line overrelaxation subject to the following convergence criterion: $\left| y_{i,j}^{n+1} - y_{i,j}^{n} \right| < 5 \cdot 10^{-6}$ for all grid points i, j, where n is the iteration level.

Once the values of y are calculated throughout the flowfield, u and v can be evaluated from (9) using second-order accurate differencing. At the lower boundary u is calculated using a second-order accurate forward scheme and v is obtained using the tangency condition and the calculated u, i.e., $v = uf'(x)$.

In order to determine p, it has been found convenient to introduce the perturbation pressure p^*, given by

$$p = -\frac{\mu}{k}x + p^*. \tag{15}$$

From (5) and (15), p^* satisfies

$$y_\psi^2 p_{xx}^* - 2y_x y_\psi p_{x\psi}^* + (1+y_x^2)p_{\psi\psi}^* = 0 \tag{16}$$

in the flowfield and Neumann conditions on the boundary, obtained by assuming (12) is valid at $x = \pm\infty$ and (13) is valid along $\psi = 0$ and $\psi = \infty$. Thus it is easily seen that p^* satisfies

$$\begin{aligned} p_x^* &= 0, && \text{at } x = \pm\infty, \\ p_\psi^* &= 0, && \text{at } \psi = \infty, \\ p_\psi^* &= -f'(x), && \text{at } \psi = 0. \end{aligned} \tag{17}$$

Equation (16) is central differenced, with its coefficients calculated from the converged values of y, and the solution is obtained for p^* using successive line overrelaxation. The values of p^* at the boundary are calculated after every iteration by defining p^* at the boundary in terms of its values at internal grid points via first-order accurate one-sided differencing of (17). The iterative procedure is repeated until convergence on p^*, where the convergence criterion used is the same as that satisfied by y.

5. Results and discussion

Numerical solutions have been obtained when the lower boundary is given by

$$f_1(x) = \begin{cases} 0.2\,[0.25 - x^2]^{1/2}, & -0.5 \leqslant x \leqslant 0.5, \\ 0, & x < -0.5 \text{ or } x > 0.5, \end{cases}$$

$$f_2(x) = -f_1(x),$$

$$f_3(x) = \begin{cases} 0.1\,[1-2x][1-4x^2]^{1/2}, & -0.5 \leqslant x \leqslant 0.5, \\ 0, & x < -0.5 \text{ or } x > 0.5, \end{cases}$$

where the points $x = 0.5$ and $x = -0.5$ are chosen to fall between grid points.

The results in the present work are based on the computational domain defined by $0 \leqslant \psi \leqslant 2$, $-4 \leqslant x \leqslant 4$, although $-2 \leqslant x \leqslant 2$ and $-6 \leqslant x \leqslant 6$ were also tested. The extent of the

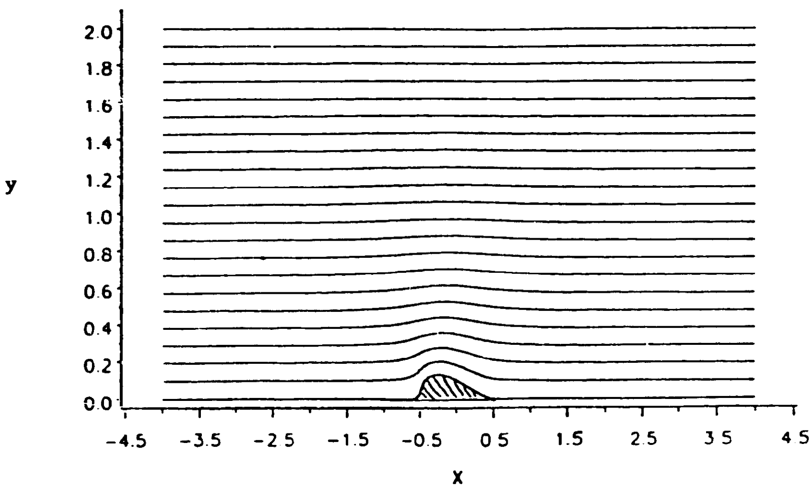

Fig. 1. Streamline pattern in the porous medium with a "Joukowski" bump, $y = f_3(x)$, along the lower boundary.

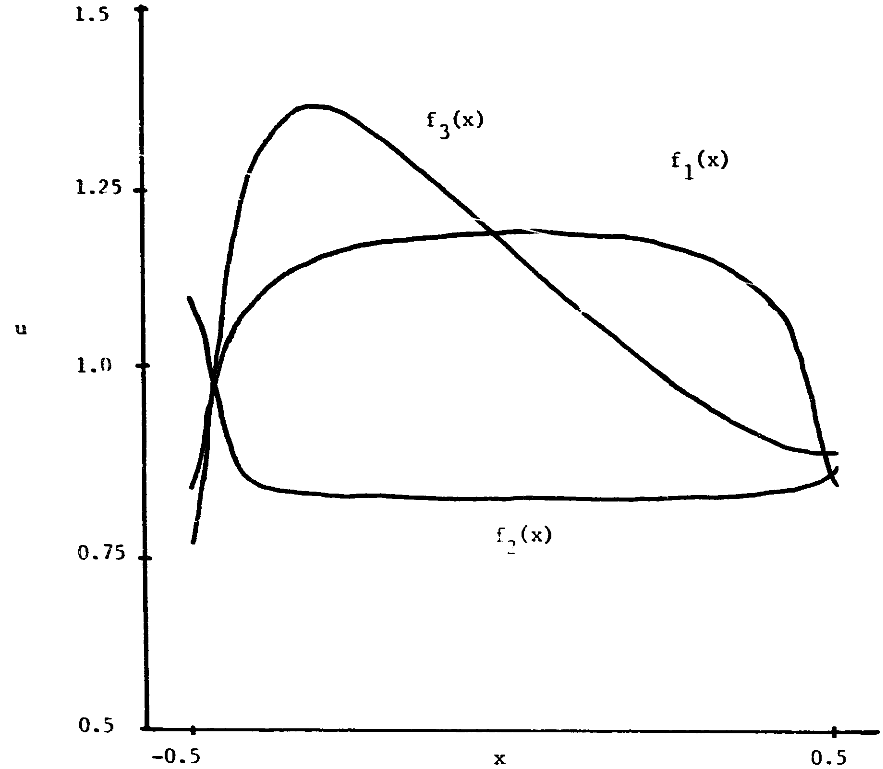

Fig. 2. Horizontal velocity component along the lower boundary for different $f(x)$.

domain in the ψ-direction has proven to be satisfactory as illustrated in Fig. 1, which demonstrates streamlines of the flow when the lower boundary is given by $f_3(x)$ and shows that the streamlines at infinity straighten out. Figure 1 also indicates the acceptable extent of the domain in the x-direction since the streamlines at $x = -4$ and at $x = 4$ appear to be straight and thus reflect the boundary conditions employed. Although the choice $-2 \leqslant x \leqslant 2$ reflected a similar behaviour, a larger computational domain has proven to be necessary when solving the perturbation pressure equation. This is due to the fact that although the dimensionless u-velocity component is taken to be unity at $x = \pm 2$, the calculated values of this velocity component along $x = 2$ are less than unity. Part of this discrepancy is ascribed to round-off errors and errors due to the accuracy of the differencing scheme, but also suggests that the extent of the computational domain might not be large enough to correctly impose the boundary conditions on p^*. The results obtained using $-4 \leqslant x \leqslant 4$ and $-6 \leqslant x \leqslant 6$ are close to each other and, to achieve relatively fine grid calculations, the range $-4 \leqslant x \leqslant 4$ is employed in the current calculations. Convergence of the solution, in terms of increasing accuracy with which the continuity equation is satisfied, has been achieved for fine grids. Our results are based on a 122×22 grid.

Figure 2 illustrates the horizontal slip velocity component at the lower boundary along the nonzero parts of $f_1(x)$, $f_2(x)$ and $f_3(x)$, showing the symmetry of this component for $f_1(x)$ and $f_2(x)$. The maximum values of this component occur at around the maxima of the functions defining the lower boundary and the minima occur at the minima of the functions.

The u-component of velocity along the vertical lines passing through points around the

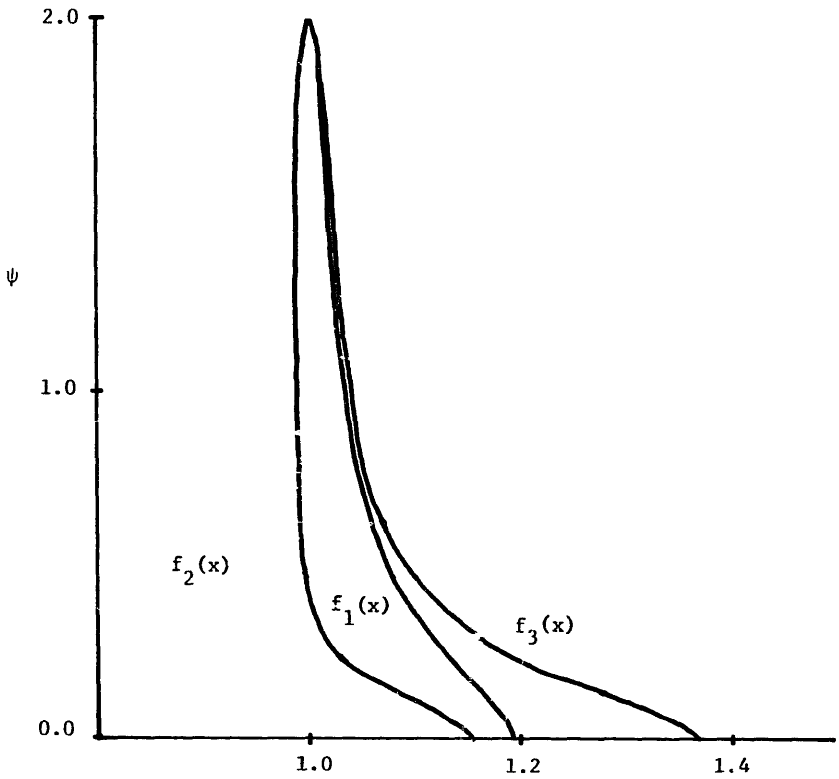

Fig. 3. Horizontal velocity component at $x = x_m$, corresponding to position of maximum thickness of $f_i(x)$.

maxima of the functions are illustrated in Fig. 3, which demonstrates the decrease in these components as we move away from the lower boundary. Although the decrease is drastic in the regions closer to the lower boundary, the components are seen to assume more uniform profiles of almost constant values in the upper parts of the domain. This conclusion is consistent with the well-known flow structure when Darcy's law is used.

In Fig. 4 the vertical slip velocity component at the lower boundary is illustrated over the nonzero part of the above functions and shows that the maximum values of this component occur at the minima of the functions and the minimum values occur at the maxima of the functions.

The perturbation pressure along the lower boundary over the nonzero parts of the functions is illustrated in Fig. 5.

6. Conclusions

The applicability of the von Mises coordinates in the study of fluid flow through porous media has been tested. This method, which is known to be useful in the numerical treatment of fluid flow over arbitrary bodies, has been employed in this work to numerically study flow

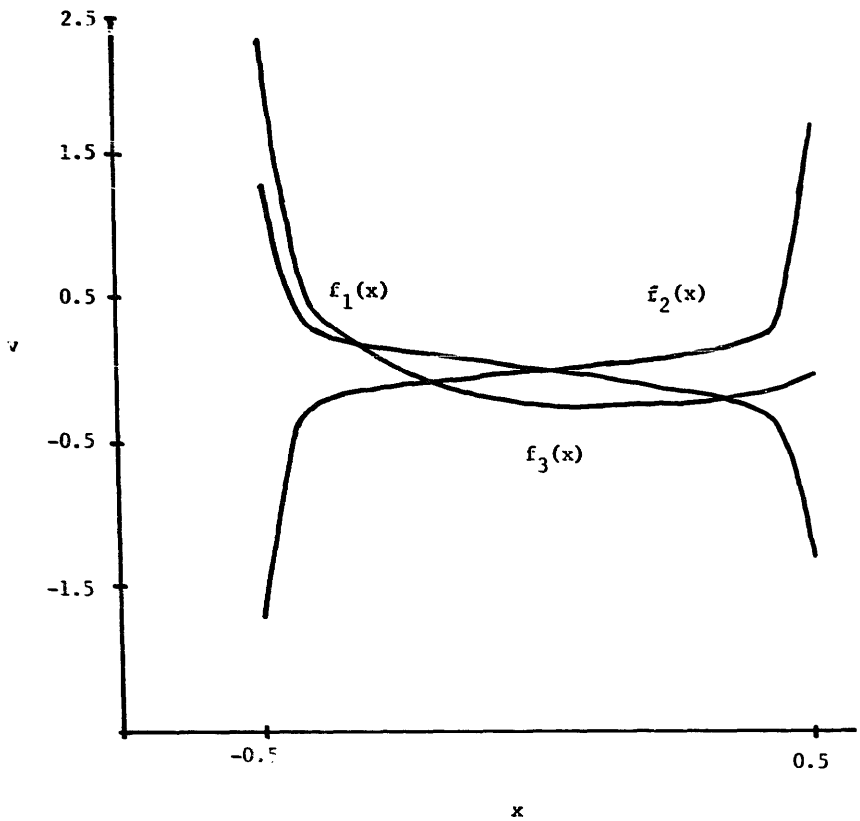

Fig. 4. Vertical velocity component along the lower boundary for different $f(x)$.

through porous media when the flow is governed by Darcy's law. The velocity components and pressure have been determined throughout the flow domain and on the curved lower boundary.

Appendix

In this Appendix we derive expressions for the derivatives associated with the time-dependent von Mises transformation, defined by

$$x = \phi, \qquad y = y(\phi, \psi, \tau), \qquad t = \tau. \tag{A.1}$$

The spatial Jacobian is given by (8) while the temporal Jacobian is

$$J^* = \frac{\partial(x, y)}{\partial(\phi, \tau)} = y_\tau. \tag{A.2}$$

Applying the chain rule to the functions x, y and t yields

$$\psi_t = -\frac{y_\tau}{y_\psi} = -\frac{J^*}{J}, \qquad \psi_x = -\frac{y_\phi}{y_\psi} = -\frac{y_\phi}{J}, \qquad \psi_y = \frac{1}{y_\psi} = \frac{1}{J}. \tag{A.3}$$

Hence first partial derivatives in the two systems are related by

$$\partial_t = \partial_\tau - \frac{y_\tau}{y_\psi}\partial_\psi, \qquad \partial_x = \partial_\phi - \frac{y_\phi}{y_\psi}\partial_\psi, \qquad \partial_y = \frac{1}{y_\psi}\partial_\psi. \tag{A.4}$$

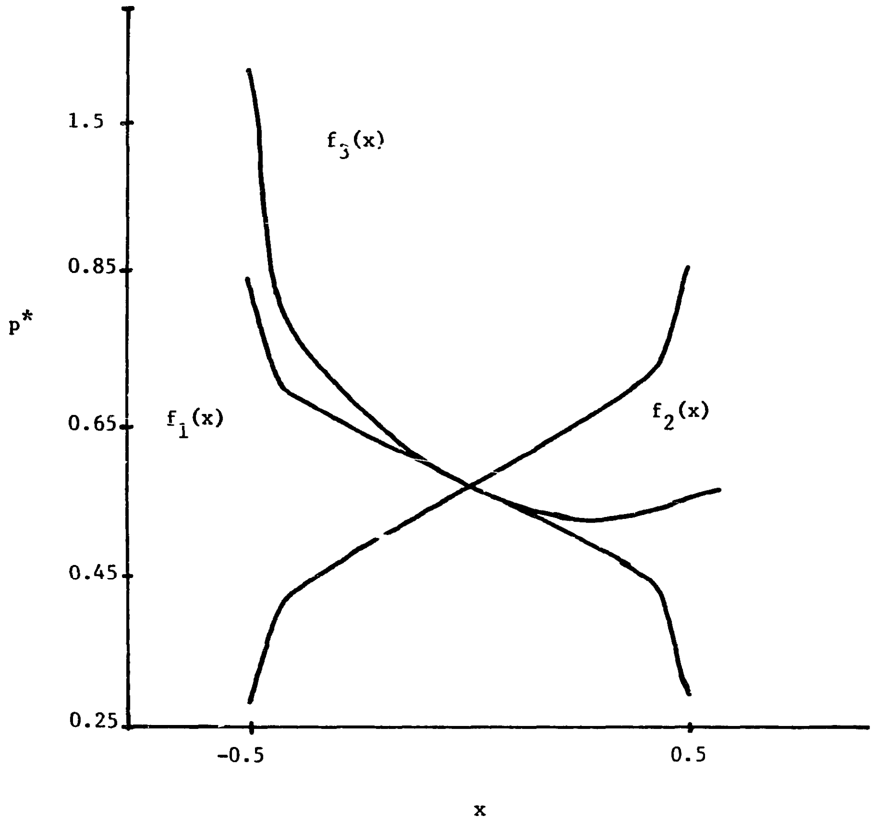

Fig. 5. Perturbation pressure along the lower boundary for different $f(x)$.

Repeatedly applying these operators, one can easily show that the Laplacian operator is given by

$$\partial_{xx} + \partial_{yy} = y_\psi^2 \, \partial_{\phi\phi} - 2 y_\phi y_\psi \, \partial_{\phi\psi} + \left(1 + y_\phi^2\right) \partial_{\psi\psi}. \tag{A.5}$$

The time-independent transformation is recovered from these results by taking $\partial_\tau \equiv 0$.

References

[1] R.M. Barron, Computation of incompressible potential flow using von Mises coordinates, *Math. Comput. Simulation* **31** (3) (1989) 177–188.

[2] G. Chavent and J. Jaffré, *Mathematical Models and Finite Elements for Reservoir Simulation*, Stud. Math. Appl. **17** (North-Holland, Amsterdam, 1986).

[3] Y.C. Fung and H.T. Tang, Solute distribution in the flow in a channel bounded by porous layers (A model of the lung), *J. Appl. Mech* **97** (1975) 531–535.

[4] M. Harr, *Groundwater and Seepage* (McGraw-Hill, New York, 1962).

[5] M.H. Martin, The flow of a viscous fluid. I, *Arch. Rational Mech. Anal.* **41** (1971) 266–286.

[6] M. Muskat, *Flow of Homogeneous Fluids through Porous Media* (McGraw-Hill, New York, 1937).

[7] G. Neale and W. Nader, Practical significance of Brinkman's extension of Darcy's law: Coupled parallel flows within a channel and a bounding porous medium, *Canad. J. Chem. Engrg.* **52** (1974) 475–478.

[8] A.E. Scheidegger, *The Physics of Flow through Porous Media* (Univ. of Toronto Press, Toronto, 3rd. ed., 1974).